J. Fluid Mech. (1999), *vol.* 391, *pp.* 319–336. Printed in the United Kingdom

Competition between distributed and localized buoyancy fluxes in a confined volume

By M. G. WELLS, R. W. GRIFFITHS AND J. S. TURNER

Research School of Earth Sciences, Australian National University, Canberra 0200, Australia

(Received 21 April 1998 and in revised form 17 February 1999)

We investigate the convection and density stratification that form when buoyancy fluxes are simultaneously applied to a finite volume in both a turbulent buoyant plume from a small source and as a uniform heat flux from a horizontal boundary. The turbulent plume tends to produce a stable density stratification, whereas the distributed flux from a boundary tends to force vigorous overturning and vertical mixing. Experiments show that steady, partially mixed and partially stratified states can exist when the plume buoyancy flux is greater than the distributed flux.

When the two fluxes originate from the same boundary, the steady state involves a balance between the rate at which the mixed layer deepens due to encroachment and vertical advection of the stratified water far from the plume due to the plume volume flux acquired by entrainment. There is a monotonic relationship between the normalized mixed layer depth and flux ratio R (boundary flux/plume flux) for $0 < R < 1$, and the whole tank overturns for $R > 1$. The stable density gradient in the stratified region is primarily due to the buoyancy from the plume but is strengthened by a stabilizing temperature gradient resulting from entrainment of heat into the plume from the mixed layer. This result may be relevant to the upper oceans of high latitude where there is commonly a destabilizing heat flux from the sea surface as well as more localized and intense deep convection from the surface.

For the case of fluxes from a plume on one boundary and a uniform heat flux from the opposite boundary the shape of the density profile is that given by the Baines & Turner (1969) 'filling-box' mechanism, with the gradient reduced by a factor $(1 + R)$ due to the heating. Thus, when $R < -1$ there is no stratified region and the whole water column overturns. When $0 > R > -1$, the constant depth of the convecting layer is determined by a balance between buoyancy and turbulent kinetic energy in the outflow layer from the plume.

1. Introduction

A destabilizing buoyancy flux distributed uniformly over the top or bottom horizontal boundary of a fluid layer drives turbulent convection in the layer when the Rayleigh number is large, and the convection maintains a nearly homogeneous layer. A localized source of buoyancy, on the other hand, produces a plume and, if the Reynolds number is large enough, the motion is again turbulent. Baines & Turner (1969) showed that a turbulent plume in a fluid volume of finite vertical and horizontal extent leads to the development of a stable density stratification. Hence if a layer is subjected to both a uniformly distributed boundary flux and an intense, localized

flux, there is a competition between the tendency for the uniform flux to overturn the layer and the tendency for the turbulent plume to stratify the system.

In a semi-enclosed sea, for example, the heat loss or evaporation from the surface may supply a buoyancy flux broadly over the surface, driving convection in a surface mixed layer. If the surface fluxes are more intense in a relatively small region, deep convection may occur, involving sinking and horizontal entrainment similar to that in the idealized turbulent plume from a small (or even point) source. Stratification may be established by the plume deep in the water column, while the surface flux maintains the upper convecting layer.

Baines & Turner (1969) have discussed the case of a turbulent plume in detail. The plume rises through its surroundings until it reaches the opposite boundary, where it spreads out in a layer of thickness h. The first water in the plume to reach this boundary is lighter than the surroundings and forms a density step. As the plume flow continues, entrainment of surroundings into the plume ensures that the outflow continually decreases in density while the density step, or 'first front', is slowly displaced downward to asymptotically approach the level of the plume source. Thus the box is slowly filled with a density gradient, the shape of which is controlled by the entrainment into the plume. This is illustrated in figure 1.

Worster & Huppert (1983) approximated the entrainment equations to obtain an analytic solution for the time evolution of the density gradient. They showed that below the first front the density gradient quickly reaches that of the steady state, an observation that agrees well with experiment. Manins (1979) extended the description of the 'filling-box' process and set limits on the aspect ratio of the box for inertial recirculation driven by the momentum of the plume outflow to be avoided. For tanks of aspect ratio > 1 the whole tank is characterized by vertical accelerations comparable to horizontal accelerations and the tank remains mixed. Baines & Turner (1969) and Barnett (1991) both concluded that the outflow depth increases with the aspect ratio, for an aspect ratio $H/r > 1$, where H is the tank depth and r is an effective tank radius.

For small aspect ratios (wide basins) Manins (1979) found that the outflow occupies $\frac{1}{4}$ of the total depth of the plume fall. However, due to the lack of any strong gradients in this region, the outflow makes little difference to the asymptotic density gradient. Manins defined a Froude number for the flow and showed that when the outflow thickness is small (as assumed by Baines & Turner 1969) the flow entrains fluid from above causing the outflow to deepen until it reaches an equilibrium depth.

Other studies relevant to the present problem have shown that when there is a pre-existing gravitationally stable density gradient in the water and a destabilizing heat flux is imposed at a horizontal boundary, a mixed layer forms and increases in depth with time. Turner (1973) and Manins & Turner (1977) showed that a balance of the kinetic and potential energy involved in the mixing process gave a convecting layer depth with the time evolution $h \propto t^{1/2}$. Deardorff, Willis & Stockton (1980) investigated the mechanism of the convective mixing process as a function of a Richardson number, defined as $Ri = g\delta\rho\Delta h/(w^*)^2$, where g is gravity, $\delta\rho$ is the density difference, w^* the r.m.s. eddy velocity of the convective motion that penetrates a distance Δh into the overlying stratification. They found that even for slowly encroaching mixed layers with high Ri the normalized interface thickness $\Delta h/h$ had a significant thickness.

When a layer is subjected to both a destabilizing uniform boundary flux (say, through the base) and a localized flux, we expect the competition between overturning and stratification building to depend on the relative strengths of the two sources and

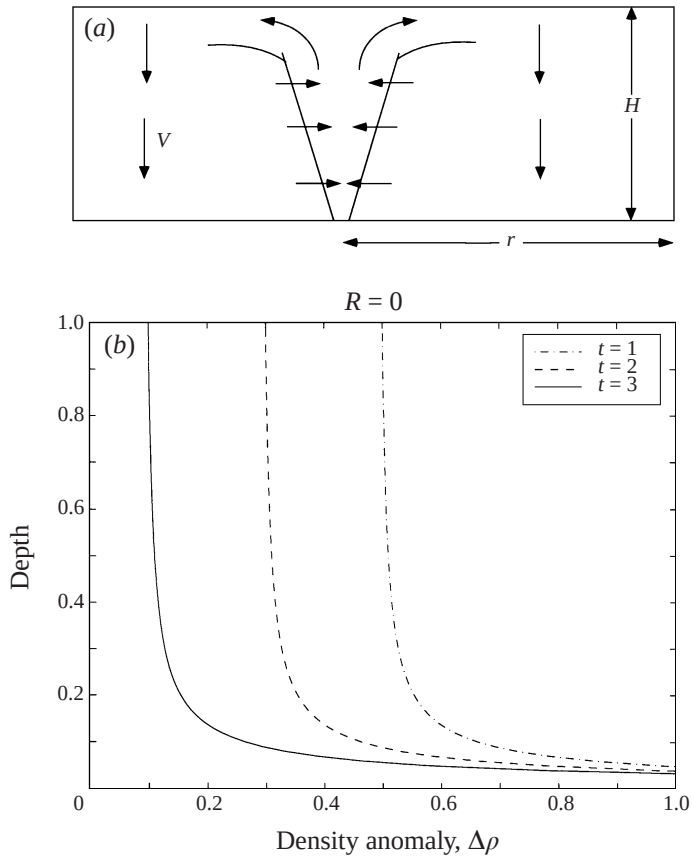

FIGURE 1. (*a*) A diagram of the filling-box model of Baines & Turner (1969), showing the entrainment of material by the plume and vertical advection V in the box. (*b*) The density profiles that result at three succesive times. The density profile remains a constant shape while decreasing linearly at every point.

the nature of the box aspect ratio. We define R to be the ratio of the integrated buoyancy flux B through the base to the buoyancy flux F from the localized source,

$$R = \frac{B}{F}, \tag{1.1}$$

and investigate the behaviour of the system as a function of R in the long-time limit. We make use of laboratory experiments in which a basal heat flux is applied to a box of water while the plume is driven by either a small source of dense salt solution at the top or a source of less-dense fresh water at the base. Of particular interest is whether a steady mixed depth can exist in which a part of the water column is well-mixed and a part is stratified. Although the use of heat and salt leads to some weak double-diffusive effects in some of the experiments, there are practical constraints in the laboratory which make the two-component experiments more convenient. In § 2 we attempt to predict the behaviour when the fluxes are released from the same horizontal boundary and, in § 3, when they are released from opposite boundaries. The experiments are described in § 4 and the experimental results are compared with the theoretical hypotheses in § 5 and § 6. A discussion of geophysical applications is presented in § 7.

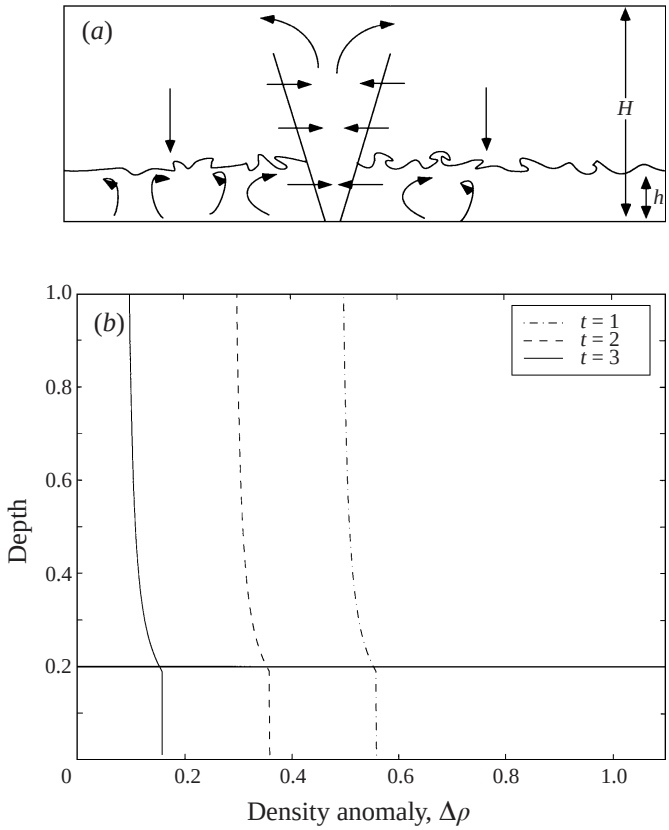

FIGURE 2. A diagram of (*a*) the expected flow pattern, with a mixed layer depth h and (*b*) density profiles that result at three succesive times, for heating from the bottom boundary and a relatively fresh-water plume source at the base. Here $R = 0.2$ and the horizontal line shows the expected depth to which there is mixing due to convection from the base.

2. Fluxes from the same boundary

The interaction of flows produced by two buoyancy sources at the bottom is shown diagrammatically in figure 2(*a*). The plume, upon reaching the top of the layer, generates an outflow that forces a general downwelling of water. The downwelling and entrainment of this water back into the plume produces a stable stratification. However, the density gradient produced by the plume, if it were not continuously replenished, would be overturned by the basal heating at a rate that can be calculated by applying the theory developed in Manins & Turner (1977). In the present situation we hypothesize that a constant convecting layer depth (less than the total depth of water) can exist when the rate at which the top of the convecting layer is advected downwards by the plume-induced circulation is experimentally equal to the rate of deepening of the convecting layer by bottom heating. If there exists such a balance, the system will consist of a well-mixed layer of depth h and an overlying density profile similar to that sketched in figure 2(*b*). Since the two buoyancy sources provide a non-zero net flux into the chamber the density everywhere must decrease linearly with time.

2.1. *Mixed layer depth determined from the buoyancy fluxes*

The depth, h, of the convecting layer can be determined by requiring that the density change at the same rate in both the stratified and convecting regions, and by assuming that the interface depth is stationary.

A complete buoyancy flux balance for the two layers is given by the pair of equations

$$\frac{\mathrm{d}\rho_{stratified}}{\mathrm{d}t} = \frac{\rho F}{A(H-h)g} - B_i + Q\Delta_s, \tag{2.1}$$

$$\frac{\mathrm{d}\rho_{mixed}}{\mathrm{d}t} = \frac{\rho B}{Ahg} + B_i - Q\Delta_s, \tag{2.2}$$

where A is the base area, H is the water depth, g is the gravitational acceleration and F is the buoyancy flux from the plume. B_i is the buoyancy flux due to entrainment of overlying stratified material, Q is the volume flux of the plume and Δ_s is the buoyancy step across the interface between the stratified and convecting regions. The two terms B_i and $Q\Delta_s$ give an indication of the relative importance of entrainment or encroachment at the interface. For either of these terms to be non-zero there must be a density step at the interface. If there is no density step, then there is a continuous transition between the two regions and there will be no additional flux of density across the interface. If the interface is stationary the entrainment buoyancy flux B_i is necessarily equal to the volume flux times the density step $Q\Delta_s$. Assuming that the rate of density change is the same in both layers, (2.1) and (2.2) imply that

$$\zeta_{mixed} = \frac{R}{1+R}, \tag{2.3}$$

where $\zeta_{mixed} = h/H$ the normalized mixed depth. The rate of density change at all levels in the tank will simply be given by the total input of buoyancy into the tank,

$$\frac{\mathrm{d}\rho}{\mathrm{d}t} = \frac{\rho F(1+R)}{AHg}. \tag{2.4}$$

The density profile is uniform in the mixed layer and of the form given by Baines & Turner (1969) in the stratified region.

Although our discussion concerns a plume from a point source, the result (2.3) will apply equally well to a plume from a line source, to periodically released thermals from a point source or to multiple point sources.

2.2. *Entrainment–advection balance*

Another way of considering how a constant mixed layer depth is formed is to look at the competition between advection and entrainment at the interface. If the convecting layer depth h is to be constant, then the rate of convective deepening, $U = \mathrm{d}h/\mathrm{d}t$, of the mixed layer must be equal and opposite to the downwelling velocity, V, of the stratified interior. Entrainment will tend to increase the mixed layer thickness while the filling-box advection tends to decrease it. When these processes are not in balance, due to either a small perturbation or initial conditions, the unequal advection and entrainment will act to drive the interface position towards the steady position.

We can determine U from Manins & Turner (1977), who derived a result for the time evolution of h for a convectively mixed layer beneath a constant density gradient as

$$h = \sqrt{6E^*}\left(\frac{B}{A}\right)^{1/2} N^{-1}t^{1/2}, \tag{2.5}$$

where $N = [(g/\rho)(\mathrm{d}\rho/\mathrm{d}z)]^{1/2}$ is the buoyancy frequency. The value of the mixing efficiency constant, E^*, is related to the fraction of the kinetic energy of the convecting layer which is converted into potential energy by mixing less-dense overlying water downward in to the mixed layer. If there is extensive penetrative convection and entrainment creating a sharp density step at the top of the convecting layer, then all the deepening is due to work of the convective motions against buoyancy forces and $E^* = 1$. On the other hand, if convection is less vigorous and the density profile remains continuous, mixed-layer deepening is by 'encroachment' only (heating of the mixed layer) and $E^* = \frac{1}{3}$. We allow N to be a function of depth in (2.5), giving

$$U = 3E^* \frac{B}{A} N(z)^{-2} h^{-1}, \tag{2.6}$$

where $N(z)$ is now the depth-dependent buoyancy frequency.

Changes of the density in the filling-box stratification are due only to vertical advection (Baines & Turner 1969) so that

$$\frac{\partial \rho}{\partial t} = -V \frac{\partial \rho}{\partial z}. \tag{2.7}$$

Since the density profile has a constant shape at large times the density changes with time everywhere at the same rate, determined by the rate of addition of buoyancy to the chamber (2.4). Hence (2.7) becomes

$$V = -\frac{\rho F(1+R)}{gAH} \left(\frac{\partial \rho}{\partial z} \right)^{-1}. \tag{2.8}$$

Setting $U = -V$ for a steady mixed layer depth gives

$$\zeta_{mixed} = \frac{R}{1+R} 3E^*. \tag{2.9}$$

If mixing into the convecting layer is due to encroachment alone we have $E^* = 1/3$ (Manins & Turner 1977) and $\zeta_{mixed} = R/(1+R)$, as was found in (2.3). The relationship between E^* and k (the ratio of the downward buoyancy flux due to entrainment B_i to the buoyancy flux from the boundary B), was found by Manins & Turner (1977) to be

$$E^* = \tfrac{1}{3}(2k+1); \tag{2.10}$$

k has been found (Denton & Wood 1981) to empirically depend upon the Richardson number and Péclet number as

$$k = \frac{0.20Ri}{1 + 0.41Ri^{3/2}} + \frac{0.18Ri}{Pe}. \tag{2.11}$$

There is a maximum value of $k = 0.2$ when $Ri \approx 1$ for high Pe, and for large Ri $k \to 0$. The values of Ri in our experiment indicate that k is likely to be small, so that there is little entrainment of buoyancy across the interface due to entrainment from the convective layer. Using (2.11) we see that E^* is a function of Richardson number and varies between $E^* = \frac{1}{3}$ for high Ri and a maximum of $E^* = 0.46$ for low Ri when the interface is entraining. Equation (2.9) is again a general result for any plume source in a confined region; the exact form of the plume is important only in terms of evaluating the exact density gradient to determine E^*.

Using the idea of the entrainment–advection balance we can also determine what a characteristic time for the system to converge from initial conditions to the steady mixed depth will be. If the system starts from a configuration where convection

initially dominates then when the plume is started a front will develop that is advected downwards until the steady depth h is reached. From Baines & Turner (1969) the time it takes the position of the first front to reach a distance z from the opposite boundary for a point source plume is given as

$$t = \frac{5}{4\alpha}\left(\frac{5\pi}{18\alpha}\right)^{1/3} r^2 H^{-3/2} F^{-1/3}\left[\left(\frac{H}{H-z}\right)^{2/3} - 1\right], \tag{2.12}$$

where α is an experimentally determined entrainment constant equal to 0.1 and r is the effective tank radius. Substituting the value of h appropriate for the steady mixed depth at a particular value of R gives a time scale on which the system converges to the steady mixed depth. Similarly if the plume was started before the basal heating, the tank would be stratified and the system would converge to the steady mixed depth on a time scale determined from (2.5) where $N(z)^2$ is the stratification produced by the filling-box process, given by (2.17).

2.3. *Interface thickness*

At the interface between the convectively mixed layer and the stably stratified region there must be a transition region in which convective elements have penetrated and partially mixed the density gradient. The thickness of this interface, Δh, is a function of a Richardson number and adds to the apparent depth of the convecting layer when it is viewed in terms of convective motion or small-scale refractive index density gradients. Hence (2.9) or (2.3) under-estimates the total depth of the mixed layer. In order to estimate the thickness of the interface we consider the average kinetic energy of heated convective elements in the turbulent mixed layer. Experimental studies (Deardorff *et al.* 1980) indicate that at low Ri the empirical relationship is

$$\frac{\Delta h}{h} = 0.21 + 1.31 Ri^{-1}, \tag{2.13}$$

derived as a curve fit to experimental data, valid for the range $5 < Ri < 40$.

This means that the observed mixed depth ζ will be greater than that given by (2.3) by

$$\zeta_{mixed} = (1.21 + 1.31 Ri^{-1})\frac{R}{1+R}. \tag{2.14}$$

In our experiments, a gradient form of the Richardson number can be defined as

$$Ri_g = \frac{N^2}{(w_*/\Delta h)^2}, \tag{2.15}$$

with w_* the root-mean-square velocity of the convective turbulent motions. As the experiments of Deardorff *et al.* (1980) used a linear density gradient their values of Ri would be the same as if they had used Ri_g, allowing a meaningful comparison to be made between results. Experimental and theoretical work of Adrian, Ferreira & Boberg (1986) has determined that

$$w_* \approx 0.6\left(\frac{Bh}{A}\right)^{1/3}. \tag{2.16}$$

The buoyancy frequency is taken from the filling-box solution of Baines & Turner (1969) and can be expressed as

$$N^2 = \tfrac{1}{4}(\pi)^{-2/3} F^{2/3} \alpha^{-4/3} H^{-5/3} \frac{\partial f_o}{\partial \zeta}, \tag{2.17}$$

where α is the entrainment coefficient and f_o is the non-dimensional density gradient in the filling-box as defined in Baines & Turner (1969). If we assume that $\Delta h \approx 0.2h$ and $R = \zeta/(1-\zeta)$ then the gradient Richardson number (2.15) can be written as

$$Ri_g \approx 0.69\pi^{2/3}(1-\zeta_m)^{2/3}(r/H)^{4/3}\alpha^{-4/3}\frac{\partial f_o(\zeta)}{\partial \zeta}, \tag{2.18}$$

which is weak function of the aspect ratio H/r, but a strong function of convecting layer depth, partially due to the form of $f_o(\zeta)$. For large values of ζ, Ri_g is small (~ 5) and we see a significant interface thickness.

3. Fluxes from opposite boundaries

3.1. *Qualitative description of the flow*

When the plume source is at the top boundary and heating is again at the base, the plume outflow spreads along the base, where it heats up. Thus the total buoyancy flux supplied to the water at the base of the tank is reduced by the basal buoyancy flux. When the magnitude of the base buoyancy flux is greater than that from the plume source ($R < -1$) a stable density gradient cannot develop and the whole water column overturns. When the magnitude of the distributed boundary flux B is less than that of the plume flux F ($R > -1$), a stable gradient similar to that in the filling-box solution may develop (in at least some of the water depth), but the density gradient will be reduced by the factor $1 + R$ below the strength of the gradient that would be produced by the plume alone. Since the plume buoyancy flux at each depth within the upper stratified region is unchanged, the entrainment and plume volume fluxes, hence the vertical advection velocity and shape of the density gradient, are also unchanged. This result can also be derived using the equations of Baines & Turner (1969) modified for the effect of the additional buoyancy into the outflow layer.

We predict that for $0 > R > -1$ an asymptotic state can be achieved in which the density profile has two distinct regions: a stably stratified region overlying a well-mixed layer of depth h, as illustrated in figure 3. The uniform mixed layer is maintained by the turbulence generated by shear in the plume outflow. However the advective balance that can maintain a steady mixed-layer depth in our previous case of buoyancy sources on the same boundary (§ 2) is no longer possible – both plume filling of the interior and mixing by convection in this case act to deepen the mixed layer. In the present case we recall the mechanism which limits the depth of the turbulent outflow layer of the plume when $B = 0$. Here the turbulent kinetic energy of the outflow must do work against buoyancy, and the extent of mixing is limited. When $B > 0$ the density gradient is reduced by a factor of $(1 + R)$ by the bottom heating but the available kinetic energy in the plume outflow is dependent only upon F. Thus the mixed depth will increase with R until, at $R < -1$, there is no stabilizing density gradient and the whole tank becomes well mixed.

3.2. *The shear-generated turbulent mixed layer*

The depth of the turbulent outflow from an axisymmetric plume was found experimentally to be $\zeta \approx 0.25$ (Manins 1979). With the addition of heating at the base, the turbulent kinetic energy in the outflow will be the same, controlled only by the plume buoyancy flux and the depth of water. Thus we expect that the mixed depth, ζ_m, increases monotonically from the value of $\zeta_m \approx 0.25$ at $R = 0$ to $\zeta_m = 1$ (mixing through the whole depth) when $R = -1$. Aspect ratios larger than 1 (deep, narrow

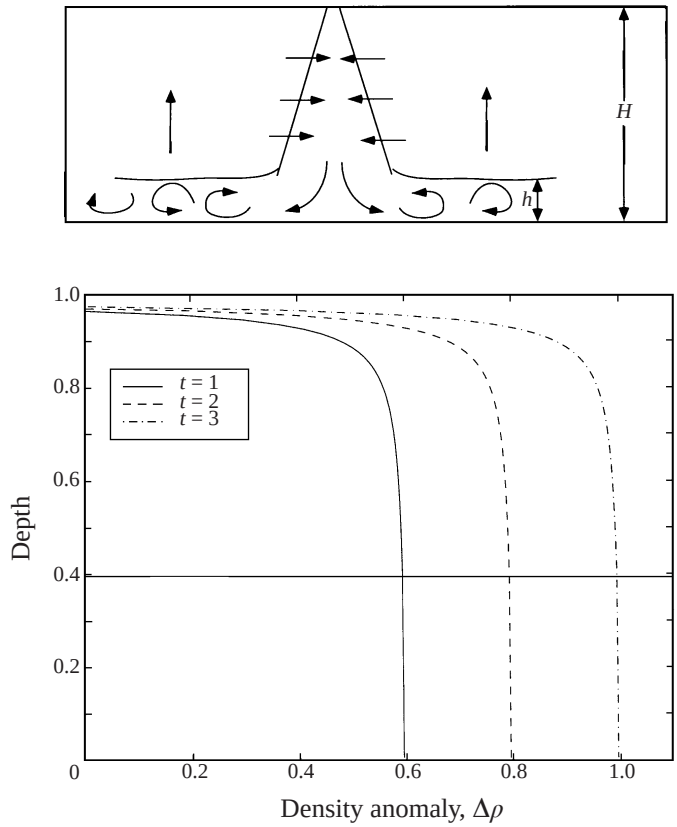

FIGURE 3. (*a*) A diagram of the flow pattern with a mixed layer depth *h*. (*b*) The expected density profiles at three succesive times for the case of a plume source at the top and heating from the bottom boundary. As the plume source is in the opposite sense to figure 2 the density increases with time and the maximum density gradient is near the top of the tank. Here $R = -0.4$ and the horizontal line shows the depth to which the plume's turbulent outflow mixes the overlying stratification.

boxes) are expected to lead to full mixing also at some $R > -1$ due to creation of a vortex recirculation at the tank wall.

The mixed depth in this case can be predicted from the total buoyancy flux per area $(B+F)/A$ and the mean outflow velocity u of the turbulent outflow layer. These provide a length scale physically analogous to the Monin–Obukhov scale (Turner 1973, 1986) as

$$L \sim \frac{-u^3}{(B+F)/A}. \tag{3.1}$$

When L is positive a relatively dense bottom mixed layer will form and when L is negative the heat input will be gravitationally unstable and a deeper mixed layer will form. As the volume flux is conserved at the base of the plume, the initial outflow velocity of the layer will be directly proportional to that of the plume, hence $u^3 \propto -F/H$. If we assume that the mixed depth scales as L in (3.1), then

$$\zeta_m \sim L/H \sim \frac{c}{1+R}, \tag{3.2}$$

where the constant of proportionality c is taken to be 0.25 to agree with observations

and theory of Manins (1979) for $R = 0$. For larger basal fluxes $|R|$ is larger and the shear mixed layer is deeper. For $R < -1$ the total buoyancy flux is destabilizing and the whole tank will overturn. It is expected that this relationship will only be valid for small R. As the magnitude of R increases, the effects of penetrative convection and the radial dependence of the outflow velocity and heating will modify (3.2). The decreasing radial velocity as the plume spreads out will be compensated by a greater uptake of heat by the slower flow, so that initially ζ_m would not change as rapidly with R as (3.2) suggests and complete overturning ($\zeta_m = 1$) will occur closer to $R = -1$.

4. Experimental design

Experiments were carried out in a square Perspex box with sides 50 cm, filled with water to a depth of between 15 and 35 cm. Base heating was provided by an electrical heating mat capable of running at powers of up to 2 kW. This was insulated from below to ensure that most of the power dissipated in the mat was transfered to the water, and overlaid by a 4 mm sheet of copper to ensure a uniform heat flux. The Perspex walls and a floating foam roof provided sufficient insulation of the water against heat loss from the water to the room. The two different water depths gave aspect ratios of approximately 0.5 and 1.

Plumes were produced either by releasing very small volume fluxes of dense salt solution at the top of the fresh water column (the opposite boundary from the heat flux) or by using a strong salt solution in the tank and releasing fresh water from a source through the centre of the base. In each case the release was at a constant rate and from tubes 7 mm in diameter. The buoyancy flux of the plume is given by

$$F = g\frac{\Delta\rho}{\rho_1}Q, \tag{4.1}$$

where Q is the volume flux and $\Delta\rho$ is the density difference between the incoming fluid and the reference density, ρ_1, of the water in the tank. Source density differences of $\Delta\rho/\rho_1 = 0.13$ to 0.18 were used, and buoyancy fluxes were typically $F = 20$ to $40\,\mathrm{cm}^4\,\mathrm{s}^{-3}$. The volume fluxes measured using a Gapmeter flow meter were sufficiently small that both the mass and momentum fluxes from the sources could be neglected. To ensure that the flow became fully turbulent when it left the nozzle we either placed cross-hairs inside the end of the tube or used a mechanical vibrator on the pipe. Experiments of Bloomfield & Kerr (1998) used very similar volume fluxes and tube diameters to generate plumes and jets, and they found over a comparable range of conditions that the virtual plume source was less than 1 cm inside the real tube source. This small correction changes the effective depth H by less than 5%.

The integrated buoyancy flux B from the base is given by

$$B = g\frac{\alpha_T J}{\rho c_p}, \tag{4.2}$$

where J is the total heat flux, α_T is the coefficient of thermal expansion of the water or salt solution (taken from data in the CRC handbook, Lide 1985) and c_p is the specific heat of the water at constant pressure (taken from data in Kaye & Laby 1973). The heat flux J was determined both from a direct measurement of the rate at which the temperature in the tank increased while it was stirred and from a measurement of the power dissipated in the heating mat. The two methods agreed well, indicating that at most 5% of the input heat was lost to the surroundings through the top, walls or base. Changes in salinity of the water within an experiment were very small, whereas

changes in temperature of the order of 10 °C were common. Hence the average value of α could change by a factor of 2 and the buoyancy flux was no longer constant for a fixed heat flux. Thus no truly steady mixed layer depth was achieved. Instead, the system reached a quasi-steady state in which the depth of the mixed layer increased as B (and $|R|$) slowly increased with time. The ratio of fluxes, R, was adjusted by changing the base heat flux.

Shadowgraph techniques were used since the sharp changes in refractive index gradient at the boundary of the turbulent region offered an easy means to measure the outflow thickness of the plume and the depth of active convection. Passive dye tracers and time-lapse recording also proved helpful in determining the mixed layer thickness by revealing regions of rapid mixing. The conductivity and temperature were measured as functions of depth (Head Precision Engineering model 5021) and the salinity and density profiles calculated from these using the polynomials of Ruddick & Shirtcliffe (1979). Profiles were taken halfway between the plume and the tank wall and it was assumed that the structure far from the plume was independent of horizontal position. Each experiment was run until the mixing depth ζ and the shape of the T, S profiles were in a quasi-steady state. As a guide it was assumed that the quasi-steady mixed depth was approached once the first front produced by the plume had been advected through 80% of the depth of the tank (Worster & Huppert 1983). This was typically 30–45 minutes after the plume was turned on, and we ran the experiments for 60–90 minutes. The majority of experiments were started with the plume and heating turned on simultaneously. Some experiments were started with one source on much earlier than the other, but the same steady mixed depth resulted after a time constant that was well described by either the advection of the first front or convective entrainment into the stratified layer above. This indicated that in the long-time limit there was no dependence upon initial conditions.

5. Experimental results for fluxes from the same boundary

The quasi-steady mixed layer depth ζ measured from shadowgraph visualization is shown in figure 4 along with the theoretical prediction of (2.14). We see that ζ varies from 0, when there is no heating, to the whole depth overturning ($\zeta = 1$) when $R \approx 1$. There is some dependence upon the aspect ratio with the narrower tank showing full depth overturning earlier than the wider tank. The weak aspect ratio dependence in (2.14) also matches the data well, with the narrower tank having a relatively deeper mixing layer than the wide tank for a given R. The uncertainties are of order 20% of h, which is roughly the thickness of the interfacial region produced by penetrative convection.

Measurements of the density profile when the steady mixed depth had been reached were made for the case of no base heating $R = 0$ and for $R = 0.4$. When there was no heating (figure 5*a*), the predicted filling-box density profile of Baines & Turner (1979) developed quickly, approaching its constant asymptotic shape and decreasing in density with time in a linear rate.

For $R = 0.4$ (figure 5*b*), we plot profiles taken after the mixed depth had reached a steady depth. When both heat and salinity are used to provide buoyancy fluxes, there will be concentration gradients of each component. However, the individual profiles will give density contributions of similar forms, both being stable above the mixed layer and near uniform in the mixed layer. A small fraction of the heat flux into the mixed layer is entrained into the plume to produce the overlying temperature profile, which produces a thermal contribution to the stable density gradient of the same

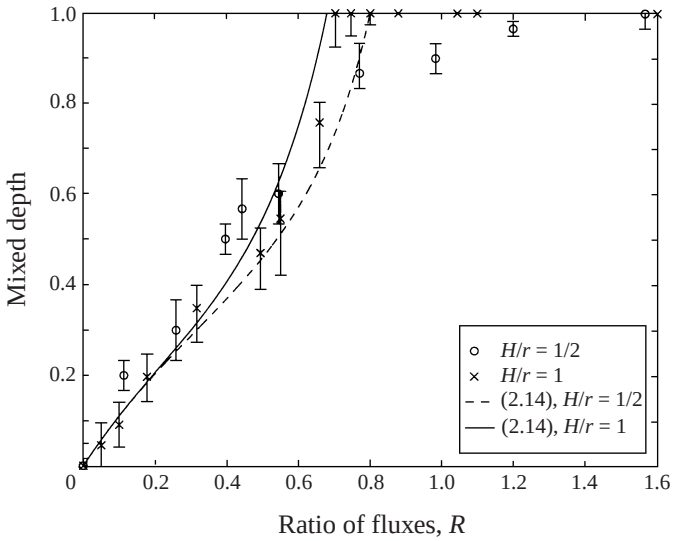

FIGURE 4. A comparison of experimental results and theory (2.14) for the steady-state mixed depth when the sources are on the same boundary, for aspect ratios of 0.5 and 1. We see that full depth mixing occurs for $\zeta \approx 1$.

form as the salinity gradient. As the flux of heat out of the base (the term $Q\Delta_s$ in (2.1)) is small relative to the input by basal heating we see a minimum in temperature just above the mixed layer.

The density profile retains a constant shape with time while decreasing linearly with time between measurements. The transition from the stratified region to the convecting region occurs at a position that agrees well with the measurements from the shadowgraph. The profiles shown are instantaneous (rather than time-averaged) and hence they ignore significant variability in the top of the mixed layer. The transition from the stratified region to the well mixed region is of order the interface thickness for the salinity profile. Due to thermal diffusion the temperature interface is about twice as thick as the salinity interface. In the stratified region, the density and salinity profiles have the same shape as in the case with no bottom heating as they are again controlled by the filling-box mechanism. However, the entrainment of heat from the convecting layer gives rise to a characteristic stable temperature gradient in the stratified region.

The use of heat and salt to provide the two buoyancy fluxes also leads to some double-diffusive effects in the experiments. For $R < 0.2$ a 'diffusive' interface formed at the top of the mixed layer and the gradient region immediately above broke down to form a second convecting layer. This second layer was relatively shallow and appeared to make little difference to the predicted mixed depth.

6. Experimental results for fluxes from opposite boundaries

When the plume was dense and descended from the top boundary, the basal heating increased the thickness of the well-mixed outflow layer. The mixed depth was measured from shadowgraphs which reveal the maximum turbulent outflow depth. The results are plotted in figure 6 and agree with the theoretical prediction of (3.2) for small R. For magnitudes of R greater than about -0.4 we do not expect the theory to agree well with experiment, and the apparent agreement is despite the expected

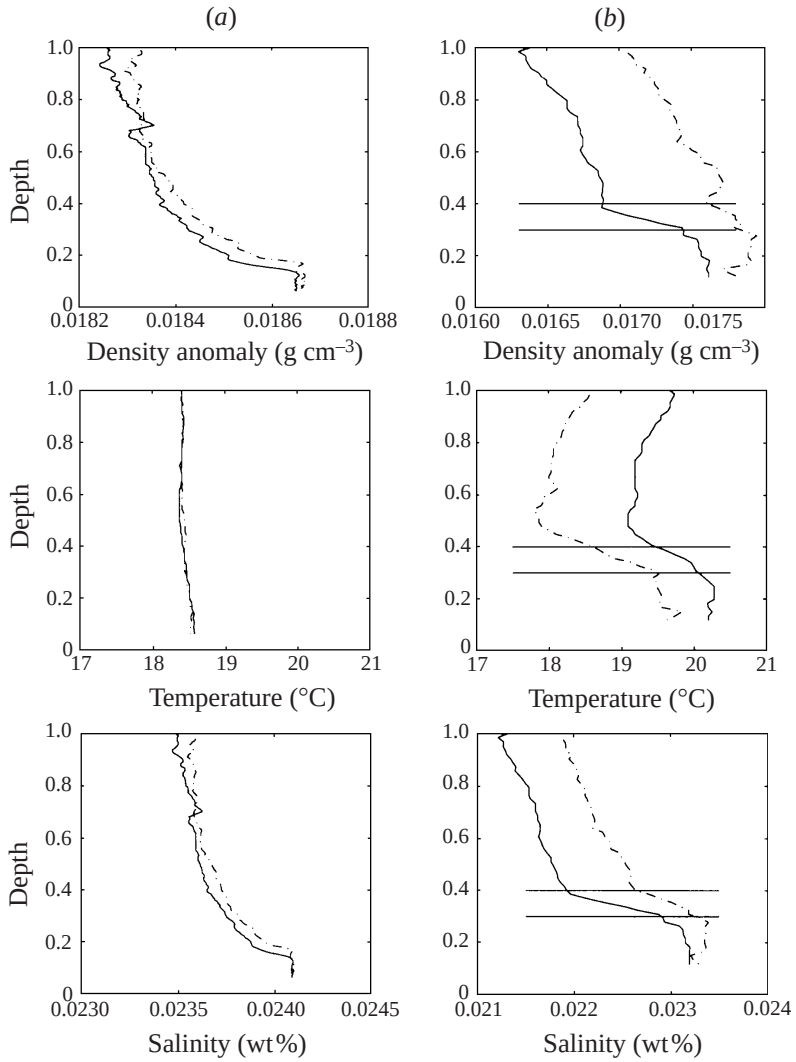

FIGURE 5. Measured density, temperature and salinity profiles at two succesive times for (*a*) $R = 0$, a normal filling-box, and (*b*) buoyancy fluxes from the same boundary and $R = 0.4$. Profiles were taken 1 minute apart in (*a*) and 5 minutes apart in (*b*). The aspect ratio is 0.5 and the horizontal lines represent upper and lower limits to the depths of convection measured independently from the shadowgraph. In both cases the density is decreasing while the profile shape remains constant.

inertial recirculation driven by the plume (Baines & Turner 1969; Barnett 1991). For the small aspect ratio full tank mixing does not occur until $R = -1$ when there is no longer any stabilizing input to the tank.

Measurements of the temperature, salinity and density profiles provide additional information. For the case of $R = 0$ we see in figure 7(*a*) that the temperature profile was uniform and the salinity distribution produced by the plume was solely responsible for the density changes. The profile has a constant shape between successive measurements while increasing linearly in density at every point. At the base the water was well mixed by turbulence to a normalized depth of 0.25 in agreement with the shadowgraph observations.

When the experiment was repeated with heating, both heat and salt gradients

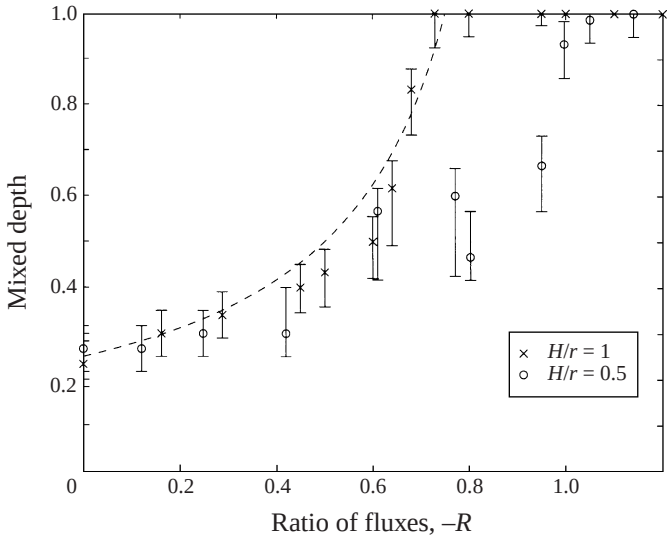

FIGURE 6. Measured mixed-layer depths in the case of distributed and isolated sources from opposite boundaries plotted against the predicted depth (3.2). Results are shown for the two tank aspect ratios.

developed and the mixed depth increased. Since the density gradients due to both temperature and salinity are produced by the plume recirculation they have exactly the same shape, but the temperature profile is destabilizing while that of salinity is stabilizing. Profiles for $R = -0.4$ are shown in figure 7(b) where the mixed layer depth has increased to $\zeta = 0.4$. Because the temperature profile is destabilizing the overall density gradient was reduced by a factor $(1 + R)$ below that in the simple filling-box process. When $R = -1$ the buoyancy fluxes were equal and opposite and the whole tank was well-mixed, giving uniform property profiles.

Double-diffusive effects were seen in the experiments only when $R < -0.7$. These took the form of up to three diffusive layers which developed above the well-mixed layer. Similar layers have been observed for a double-diffusive plume (and single buoyancy source) (McDougall 1983). While the layers did not appear to significantly influence the overall density distribution, they did make it more difficult to distinguish the top of the well-mixed layer.

7. Applications

The density structure of enclosed seas may, in part, represent the partially mixed result of competition between the tendency for deep localized convection to stratify the water column by the filling-box process on the one hand, and the maintenance of a surface mixed layer on the other. As our model is more general than for just the point source plume studied, the same result should hold if the localized buoyancy production was periodic but with the same total buoyancy flux when integrated over each cycle (Baines & Turner 1969; Killworth & Turner 1982).

Addition of rotation to the problem is expected to make only small quantitative differences to the long-term density profile and vertical advection of this very large filling-box. This is shown by Pierce & Rhines (1996) who experimentally found that for low rotation a turbulent plume generates the same density gradient as in the non-rotating filling-box. Thus while we do not find point sources in nature, we do

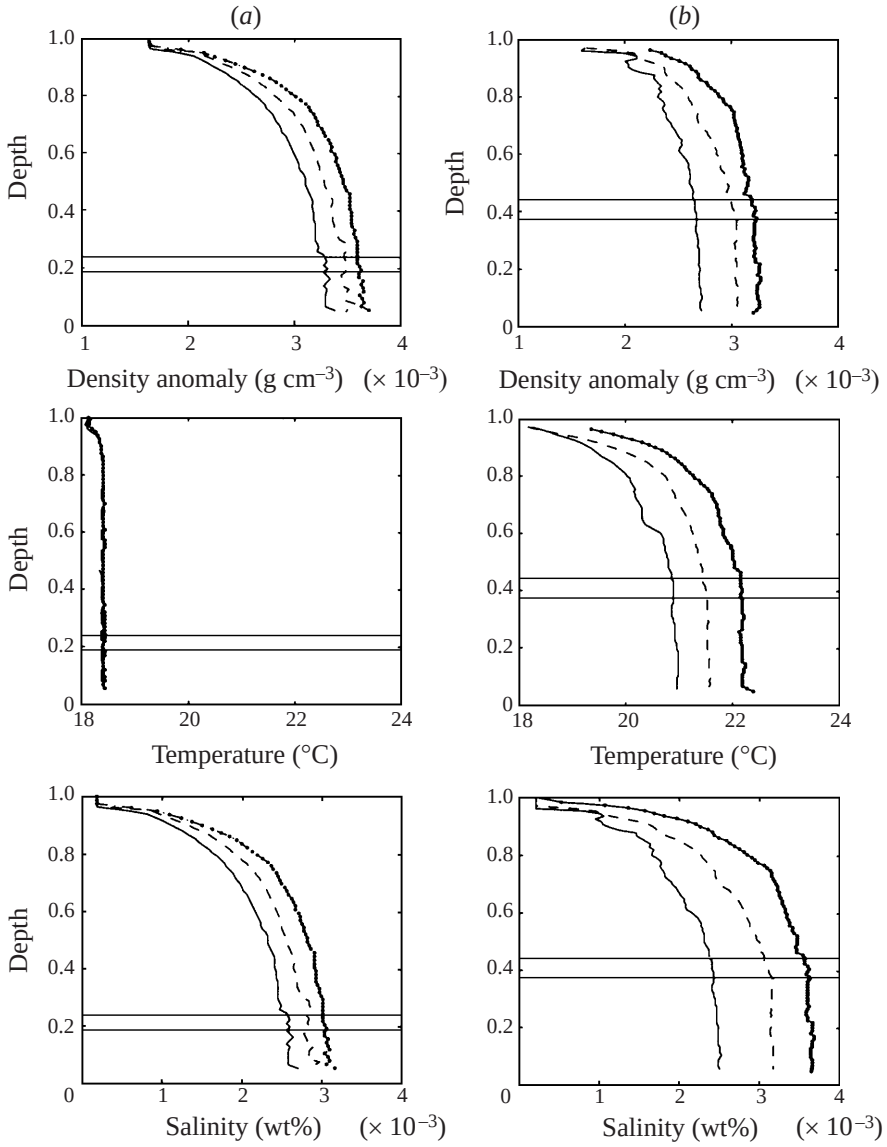

FIGURE 7. Measured density, temperature and salinity profiles at three succesive times. (*a*) $R = 0$. Since there is no heating the temperature is constant (except for small amount of surface cooling). (*b*) $R = -0.4$. The temperature profile is the same shape as the salinity profile. The normalized mixed-layer depth is 0.41 which agrees well with independent shadowgraph measurements, where the upper and lower limits of this measurement are shown by the horizontal lines. Profiles were taken 5 minutes apart in (*a*) and 10 minutes apart in (*b*). In both cases the density is increasing while the profile shape remains constant.

find periodic isolated sources of deep convection so expect our study to be indicative of processes in the ocean.

Profiles in high-latitude seas such as that from the Bering Sea, shown in figure 8, reveal a characteristic temperature profile with a maximum beneath the mixed layer, in the same way that our 'upside down' experiments show a minimum temperature above the mixed layer. The concentration profile of dissolved oxygen (an indication

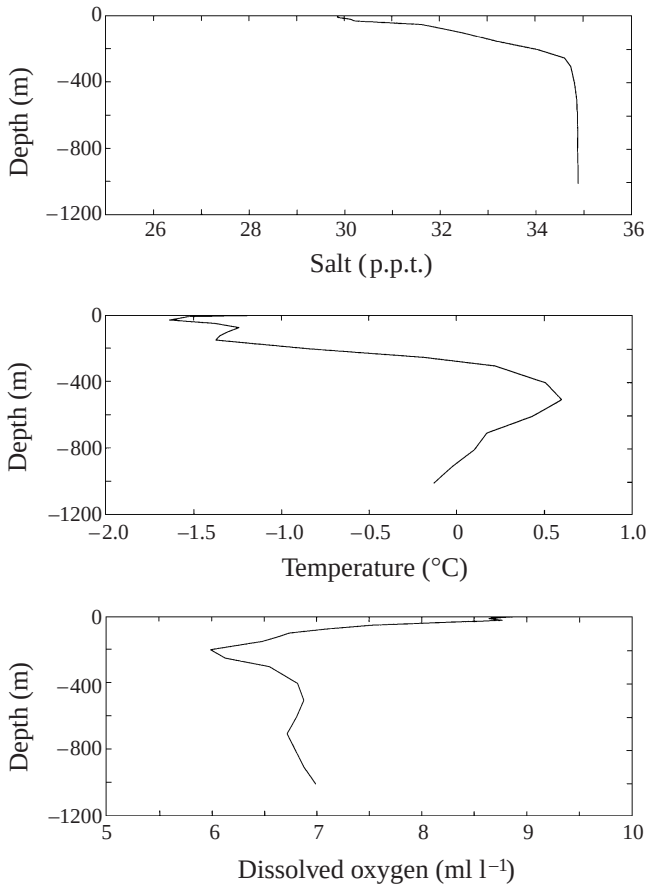

FIGURE 8. Measurements of density, temperature and oxygen profiles taken in the Bering Sea, from the Levitus (1987) oceanographic data set.

of how long the water body has been away from the surface) shows a minimum below the 'mixed' surface layer and a maximum at greater depths. Both of these effects are consistent with the circulation and stratification produced by the combined effects of deep plume-like convection and a widespread surface buoyancy flux. The weak stratification apparent within the surface layer may be a result of other factors, such as an input of fresh water at the surface from melting ice and precipitation or lateral advection of water masses. Since this sea, like most others, is not isolated from the oceans, lateral advection will lead to intrusions of warmer water into the colder Bering Sea. It is this lateral advection that is the means by which the sea can maintain steady long-term properties rather than continue to decrease in density as do our confined 'upside down' laboratory experiments.

8. Conclusions

When there is a uniform buoyancy flux through the horizontal boundary at which the plume source is located, we have shown that the long-time steady mixed depth of the finite chamber may be a partially mixed and partially stratified one, a wholly stratified one or a completely mixed one, depending on the ratio of the two buoyancy

fluxes. The partially mixed state involves a convecting layer whose depth adjusts until the rate of encroachment into the stratification is equal and opposite to the vertical advection driven by the plume filling-box process. For flux ratios $0 < R < 1$ the normalized mixed layer depth, $\zeta_{mixed} = h/H$, is $\zeta_{mixed} = (1.2 + 1.31Ri^{-1})R/(1 + R)$. For $R = 0$ the whole tank is stratified apart from the turbulent outflow from the plume and for $R > 1$ the whole of the water column is convectively stirred. Profiles in the stratified layer had the same form as in the filling-box theory of Baines & Turner (1969). Entrainment of buoyancy (heat) from the mixed layer resulted in the production of a temperature minimum (in our case with bottom heating) just above the convectively mixed layer. The transition between the well-mixed region and the stratified region has an appreciable thickness, which increases as the aspect ratio increases so in tanks having large aspect ratios overturning occurred for $R < 1$.

In a possible oceanographic application of these results concurrent widespread surface cooling or salt input due to freezing or evaporation on the one hand and deep convection due to a localized buoyancy flux on the other are predicted to lead to a steady surface mixed-layer depth. The process will also lead to a temperature maximum just below the mixed layer. The results apply equally to the cases where there is a line source or a periodic source of buoyancy in competition with a steady distributed source, as the relationships between vertical plume advection and the density gradient are the same.

When the two buoyancy fluxes were released from opposite boundaries a steady mixed depth was again observed. However, the balance of vertical advection and enchroachment, processes which now act in the same direction, could not occur. A dynamic balance applies instead. Since the fluxes were introduced at opposite boundaries, the distributed boundary flux must be added to the outflow from the turbulent plume, resulting in a filling-box density gradient proportional to the difference between the fluxes. Thus the gradient is a factor $(1 + R)$ smaller than that which would be generated by the plume alone. The reduced gradient is stable only for $R > -1$ whereas for $R < -1$ the whole tank overturns. For $R > -1$ a mixed layer forms due to the turbulent kinetic energy of the plume outflow, and has a depth determined by the extent to which the turbulent kinetic energy is able to mix the stabilizing density gradient. The mixed layer depth in this case again increases as R increases. This situation may possibly occur in the Earth's liquid outer-core, where it has been suggested (Fearn & Loper 1981; Fearn, Loper & Roberts 1981; Whaler 1980) that plumes of less-dense residual melt may be released from the solidification front at the bottom of the outer core, potentially leading to the density stratification of the outer core. The relatively uniform heat flux from the core to the base of the solid mantle provides a destabilizing buoyancy flux from the top and must tend to overturn the core. If isolated plumes do exist in the core (and we doubt this because they seem likely to have azimuthal spacings much smaller than the depth of the outer core) then our results would imply that the system should be completely mixed if the total buoyancy flux from the inner core–outer core boundary is less than the total buoyancy flux due to cooling from the top of the core ($R < -1$). On the other hand, the outer core could be partially stratified with a convecting layer (of normalized depth $\zeta \approx 0.25/(1 + R)$) at the top if the cooling to the mantle provides a lesser buoyancy flux ($R > -1$).

REFERENCES

Adrian, R. J., Ferreira, R. T. D. S. & Boberg, T. 1986 Turbulent thermal convection in wide horizontal fluid layers. *Exps. Fluids* **4**, 121–141.

Baines, W. D. & Turner, J. S. 1969 Turbulent buoyant convection from a source in a confined region. *J. Fluid. Mech.* **37**, 51–80.

Barnett, S. 1991 The dynamics of buoyant releases in confined spaces. PhD Thesis, Cambridge University.

Bloomfield, L. J. & Kerr, R. C. 1998 Turbulent fountains in a stratified fluid. *J. Fluid. Mech.* **358**, 335–356.

Deardorff, J. W., Willis, G. E. & Stockton, B. H. 1980 Laboratory studies of the entrainment zone of a convectively mixed layer. *J. Fluid. Mech.* **100**, 41–64.

Denton, R. A. & Wood, I. R. 1981 Penetrative convection at low Peclet number. *J. Fluid. Mech.* **113**, 1–21.

Fearn, D. R. & Loper, P. E. 1981 Compositional convection and stratification of the Earth's core. *Nature* **289**, 393–394.

Fearn, D. R., Loper, P. E. & Roberts, P. 1981 Structure of the Earth's inner core. *Nature* **292**, 232–233.

Kaye, G. W. C. & Laby, T. H. (Eds.) 1973 *Table of Physical and Chemical Constants*, 14th Edn. Longman.

Killworth, P. D. & Turner, J. S. 1982 Plumes with time-varying buoyancy in a confined region. *Geophys. Astrophys. Fluid Dyn.* **20** 265–291.

Levitus, S. 1987 *Climatological Atlas of the World Ocean.* Rockville, MD: NOAA.

Lide, D. R. 1985 *CRC Handbook of Chemistry and Physics*, 72nd Edn. CRC Press.

McDougall, T. 1983 Double diffusive plumes. *J. Fluid. Mech.* **133**, 321–343.

Manins, P. C. 1979 Turbulent buoyant convection from a source in a confined region. *J. Fluid. Mech.* **91**, 765–781.

Manins, P. C. & Turner, J. S. 1977 The relation between the flux ratio and energy ratio in a convectively mixed layer. *Q. J. R. Met. Soc.* **104**, 39–44.

Pierce, D. W. & Rhines, P. B. 1996 Convective building of a pycnocline: laboratory experiments. *J. Phys. Oceanogr.* **26**, 176-190.

Ruddick, B. R. & Shirtcliffe, T. G. L. 1979 Data for double diffusers. *Deep-Sea Res.* **26**, 775–787.

Turner, J. S. 1973 *Buoyancy Effects in Fluids.* Cambridge University Press.

Turner, J. S. 1986 Turbulent entrainment: the development of the entrainment assumption and its aplication to geophysical flows. *J. Fluid. Mech.* **173**, 431–471.

Whaler, K. A. 1980 Does the whole of the Earth's outer core convect? *Nature* **287**, 528–530.

Worster, M. G. & Huppert, H. E. 1983 Time dependent density profiles in a filling-box. *J. Fluid. Mech.* **132**, 457–466.